



Valorization of Geothermal Silica and Natural Bentonite through Geopolymerization: A Characterization Study and Response Surface Design

Himawan Tri Bayu Murti Petrus^{1,2*}, Muhammad Olvianas^{1**}, Widi Astuti³,
Muhammad Istiawan Nurpratama⁴

¹*Sustainable Mineral Processing Research Group, Department of Chemical Engineering, Faculty of Engineering, Universitas Gadjah Mada, Jl. Grafika No. 2 Kampus UGM Bulaksumur, Yogyakarta 55281, Indonesia*

²*Unconventional Georesources Research Center, Faculty of Engineering, Universitas Gadjah Mada, Jl. Grafika No. 2 Kampus UGM Bulaksumur, Yogyakarta 55281, Indonesia*

³*Research Unit for Mineral Technology, Indonesian Institute of Sciences (LIPI), Jl. Ir. Sutami Km. 15, Tanjung Bintang, Lampung Selatan, Indonesia*

⁴*PT. Geo Dipa Energi (Persero) Unit Dieng, Jl. Dieng RT. 01/ RW. 01, Area Industri, Sikunang, Banjarnegara, Kabupaten Wonosobo, Jawa Tengah 56354, Indonesia*

Abstract. Geothermal silica is a potential source of amorphous silica for producing geopolymer concrete. The valorization of geothermal silica as a geopolymer concrete provides an opportunity for an added value to the geothermal-based power industry. In this study, silica content, NaOH molarity, and curing temperature effect were investigated and optimized for compressive strength using response surface methodology. The effect of the single parameter on geopolymerization was qualitatively observed using Fourier transform infrared spectroscopy (FTIR) and scanning electron microscopy-coupled with energy dispersive X-ray spectroscopy (SEM-EDS). The characterization of the geopolymer samples using FTIR and SEM-EDS revealed that the aluminosilicate structure was formed in all geopolymer samples. The geopolymerization rate can be accelerated using the lower level of geothermal silica and the high level of NaOH molarity and curing temperature. Based on optimization studies, the R-square value was 99.89%. The optimum formulation was found at a silica content of 130 g, NaOH molarity of 10 M, and curing temperature of 80°C with a desirability value of 0.99. At the optimum condition, the compressive strength was calculated as 7.73 MPa.

Keywords: Bentonite; Geopolymer; Geothermal silica; Response surface design; Valorization

1. Introduction

Geopolymers can be produced by combining various solid aluminosilicate materials with a mixture of high concentrations of alkaline hydroxide and silicate solution (Hajimohammadi et al., 2008). Geopolymer possesses a three-dimensional structure that consists of an amorphous polymeric Si-O-Al framework (Hajimohammadi et al., 2010). These materials can be categorized as eco-friendly in comparison with Portland cement in terms of CO₂ emission during the production process (Duxson et al., 2007; Hajimohammadi et al., 2008). Geopolymers exhibit excellent physical properties, such as relatively high

*Corresponding author's email: bayupetrus@ugm.ac.id, Tel.: +62-81-327770497, Fax: +62-81-327770497

**Corresponding author's email: muhammad.olvianas@mail.ugm.ac.id

doi: [10.14716/ijtech.v12i1.3537](https://doi.org/10.14716/ijtech.v12i1.3537)

mechanical strength, resistance to an acid environment, and heat resistance (Nurjaya et al., 2015) and possesses low thermal conductivity (Skvara et al., 2005; Duxson et al., 2007). Having those excellent properties, geopolymer has been recognized as a promising technology to substitute conventional cement in the construction industry and as a new method to utilize industrial and radioactive waste (Xua and van Deventer, 2003). Raw materials for geopolymer synthesis are varied and include fly ash, bottom ash, natural clays, and minerals, as well as metal slags (Heath et al., 2014; Ashadi et al., 2015). Many studies have concentrated on fly ash-based geopolymer due to its chemical suitability and relative abundant availability (Zhang et al., 2012). Fly ash and metakaolinite, which are classified as calcined materials, have a faster dissolution and gelation and exhibit higher compressive strength (Xua and van Deventer, 2003; Skvara et al., 2005). Recently, there has been a new trend to use a different source of aluminosilicate precursors, instead of fly ash, for geopolymerization (Perná et al., 2014). Xua and van Deventer (2003) studied the geopolymerization process using different sources of material (kaolinite, albite, and fly ash). Mixing these source materials can produce geopolymers of a higher mechanical strength. Alshaaer (2013) showed that additional immersion of kaolinite-based geopolymer in 6 M of alkaline solution for 1 hour can modify the geopolymer surface and enhance its compressive strength. Red mud and bauxite have also been utilized as geopolymer materials (Hairi et al., 2015).

Moreover, geothermal silica can also potentially be used as a geopolymer precursor due to its reactivity. At the geothermal power plant operated by PT. Geodipa Energy in Dieng, Jawa Tengah, Indonesia, approximately 250 tons of geothermal silica (inset of Figure 1a) are removed from the process equipment, collected in sedimentation ponds, and then dumped into landfills. The study of geopolymerization using geothermal silica is still lacking. Previous studies have presented the effect of a single variable on geopolymerization using a mixture of geothermal silica-kaolinite and geothermal silica-bentonite (Olvianas et al., 2015; Petrus et al., 2016). However, the effect of combined variables and associated optimization studies have not been reported. To analyze the various factors of geopolymerization, this study adopted response surface methodology (RSM). RSM is a statistical technique for process evaluation and optimization used in industries and research fields to control process response or independent variables (Dhakal et al., 2014; Ferdana et al., 2018; Petrus et al., 2020; Januardi and Widodo, 2020). It has been used in the field of geopolymer and concrete to optimize various parameters (Dhakal et al., 2014; Şimşek et al., 2015; Gao et al., 2016; Mohammed et al., 2018). To this end, the present work was conducted to optimize the compressive strength of geopolymer material from a mixture of geothermal silica and bentonite. The combined effect of silica content, NaOH molarity, and curing temperature were investigated using a full two-level factorial design in RSM. The effect of a single variable on the chemical bond and microstructure was also observed using Fourier transform infrared spectroscopy (FTIR) and scanning electron microscopy-coupled with energy dispersive X-ray spectroscopy (SEM-EDS).

2. Materials and Method

2.1. Materials

Geothermal silica and natural bentonite (Inset of Figures 1a and 1b), as main raw materials for geopolymer synthesis, were obtained from PT. Geodipa Energy and conventional clay industries at Bayat, Klaten, Jawa Tengah, Indonesia, respectively. Sodium hydroxide pellet with 97% wt. purity was purchased from Merck Millipore (Darmstadt,

Germany). Sodium silicate solution was purchased from CV. Brataco Chemika (Yogyakarta, Indonesia).

2.2. Geopolymer Preparation

Raw materials (geothermal silica and natural bentonite) were dried, milled, and sieved through a 60-mesh screen sieve before use. Thereafter, the geothermal silica and bentonite powder were thoroughly blended with alkaline activator solution to form geopolymer paste. Alkaline activator solution was synthesized by dissolving sodium hydroxide pellets in tap water, followed by pouring the sodium silicate solution into a sodium hydroxide solution. The solution was cooled for 2 hours at room temperature. For one geopolymer sample, the total volume of the alkaline activator solution was about 55 mL, and the volumetric ratio of NaOH and Na₂SiO₃ solution was about 1:1. Geopolymer paste was cast in a cubical mold with a volume of 125 cm³. Prior to the curing process, the specimens were stored for 2 days at room temperature to solidify. After solidification at room temperature, the specimens were cured at the desired temperature (following the experimental combination values) for 8 hours. Upon the compressive test, the cured samples were cooled and kept at room temperature for 7 days. Table 1 presents the combination of independent variables for test specimens. The specimens' run code was denoted by the combination of independent variables. For example, the sample with run code AB used 140 g of geothermal silica, 10 g of bentonite, 10 M of NaOH, and 60°C of curing temperature.

Table 1 The values of independent variables

| Variables | Range and level | |
|--|------------------|------------------|
| | +1 | -1 |
| Silica content, g (X ₁) | 140 ^a | 130 ^b |
| NaOH molarity, M (X ₂) | 10 | 8 |
| Curing temperature, °C (X ₃) | 80 | 60 |

2.3. Characterization

The raw materials were analyzed by X-ray fluorescence (XRF) (Rigaku-NEX QC Quant EZ) to determine their oxide components. The crystallinity characterization was conducted using XRD (Shimadzu XRD-6000) analysis using Cu-Kα X-ray irradiation. To measure the compressive strength, the Universal Testing Machine (Torse UTM AMU-5DE) was used. FTIR (Shimadzu IR Prestige 21) analyses were used to determine the chemical bonding in the geopolymer sample using the standard KBr pellet technique. Microstructural analysis of the geopolymer was performed using SEM (JEOL JSM 6510) with an additional fixture of energy dispersive X-ray spectroscopy to observe the elemental distribution. SEM observation was operated at a voltage of 20 kV.

2.4. Design of Experiments and Statistical Analysis

RSM was employed as a statistical technique for assessing the interaction and optimization of variables; it has the advantage of reducing experimental data points. A two-level factorial design was applied with three independent variables, as displayed in Table 1, with compressive strength as the dependent variable. The polynomial equation of the correlation between the response variable and independent variables can be expressed in a general form as follows (Bezerra et al., 2008; Montgomery, 2013):

$$Y = \beta_0 + \sum_{i=1}^k \beta_i x_i + \sum_{i=1}^k \beta_{ii} x_{ii}^2 + \sum_{1 \leq i < j \leq k} \beta_{ij} x_i x_j + \varepsilon \tag{1}$$

where Y is the response, x_i and x_j are the independent variables (i and j are the range from 1 to k), β₀ is the constant coefficient, β_i, β_{ii}, β_{ij} are the coefficients for the linear, quadratic

and interaction effect, and ε represents the error. The coefficient of correlation (R^2), ranging from 0 to 1, was employed to predict the fitness of the proposed model. A highly accurate model is indicated by R^2 close to 1.

3. Results and Discussion

3.1. Raw Material Analysis

XRD analyses of the raw materials are presented in Figures 1a and 1b. The XRD pattern for geothermal silica showed a hump along 10° to 30° 2θ , which indicates that the geothermal silica possessed an amorphous phase. This result is in good agreement with published studies for rice husk ash derived-silica (Dhaneswara et al., 2020), silica fume (Ye et al., 2016) and geothermal silica waste (Gomez-Zamorano et al., 2016). On the contrary, the XRD pattern for bentonite showed several crystalline structures. Quartz (SiO_2 ; JCPDS: 96-901-3322) structures were observed at 2θ of 20.75° , 26.53° , 36.47° , 50.06° , 59.89° , and 68.07° ; nacrite ($\text{Al}_2\text{Si}_2\text{O}_5(\text{OH})_4$; JCPDS: 96-900-9231) and lazurite ($\text{Na}_3\text{Ca}(\text{Al}_3\text{Si}_3\text{O}_{12})\text{S}$; JCPDS: 96-901-1356) structures were indicated at 2θ of 12.3° , 20.13° , 24.83° , 62.18° , and 23.9° . A small portion of hematite (Fe_2O_3 ; JCPDS: 96-900-9783) phase was also found as a reflection of reddish color appearance in bentonite. Volume fraction calculation of each phase was performed using Match! software. The volume fractions of the quartz, nacrite, lazurite, and hematite phases were calculated as 50.9, 26.7, 17.9, and 4.4%, respectively. The XRD pattern of the samples revealed that raw materials have the main components for geopolymerization, that is, amorphous silica and aluminate substances. XRF analysis (Table 2) showed that the silica geothermal polymer had a high purity of SiO_2 with a concentration of 96.06% wt. Bentonite was observed as 50.99% SiO_2 and 20.01% Al_2O_3 .

Table 2 Oxide composition of geothermal silica and bentonite

| Oxides | SiO_2 | Fe_2O_3 | Al_2O_3 | K_2O | TiO_2 | CaO | SO_3 | MnO | Minor Components |
|-------------------|----------------|-------------------------|-------------------------|----------------------|----------------|--------------|---------------|--------------|------------------|
| Geothermal silica | 96.09 | 0.55 | 0.73 | 0.33 | - | 0.28 | 0.50 | - | 1.52 |
| Bentonite | 50.99 | 22.68 | 20.01 | 0.43 | 1.89 | 1.25 | 0.46 | 0.44 | 1.14 |

Based on aforementioned results, the bentonite contained a considerable amount of Fe element. During polymerization, the reactive Fe will consume the hydroxide ions and rapidly reprecipitate as hydroxide or oxy-hydroxide phases (van Deventer et al., 2007). Therefore, the unwanted Fe reaction will reduce the dissolution rate of Si-Al mineral as the main precursor for the geopolymer.

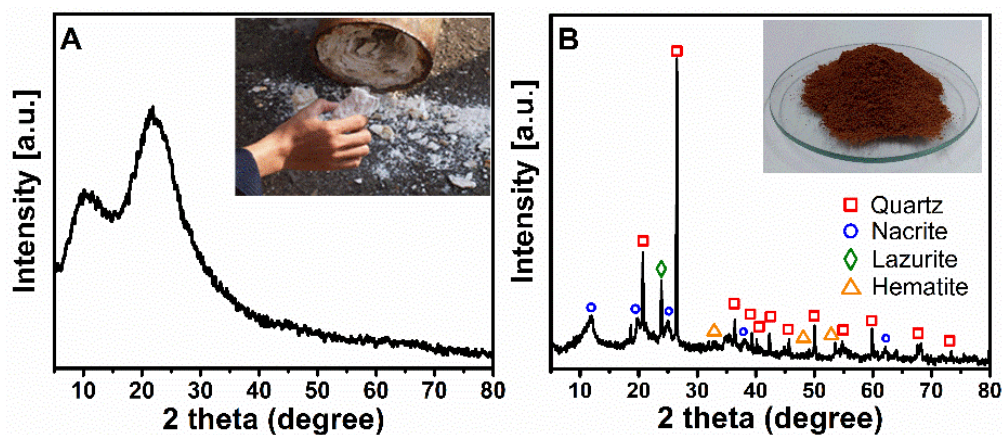


Figure 1 (a) XRD pattern of geothermal silica (inset: silica deposition inside the unused pipe); (b) XRD pattern of bentonite (inset: natural bentonite used in this study)

3.2. Fourier Transform Infrared Spectroscopy (FTIR) Analysis

The geopolymerization reaction that occurs in each specimen was studied using FTIR analysis. Figure 2 shows the full range of FTIR spectra and important absorption bands in every sample. Six absorption bands were found in FTIR analysis, as shown in Figure 2. The absorption bands in 3250–3750 cm^{-1} were observed due to the occurrence of stretching vibration of the -OH groups or bonded water. The -OH group bending vibration was also found at 1645 cm^{-1} . The geopolymer structure was clearly observed at 900–1300 cm^{-1} , which indicates the Si-O-(Si, Al in tetrahedra coordination) asymmetric stretching. Additionally, two important bands were observed at about 500–800 cm^{-1} and 400–600 cm^{-1} . These bands can be designated to the zeolitic framework. At the 500–800 cm^{-1} range, so-called pseudo-lattice vibrations, the framework possessed tetrahedral structural units and mainly consisted of SiO_4 and AlO_4 tetrahedra (Fernández-Jiménez and Palomo, 2005; Król et al., 2016). In this study, the bands at 460 and 787 cm^{-1} clearly showed that zeolite A and zeolite X were observed in geopolymer samples (Król et al., 2016). The existence of zeolite A (LTA-type zeolite) and zeolite X (FAU-type zeolite) in geopolymer material has been previously reported. Some aluminosilicates gel transformed into nanocrystalline zeolite during the curing process, indicated by the evolution of a broad peak centered at $\pm 28^\circ 2\theta$ into a sharp peaks XRD pattern (Provis et al., 2005).

In Figure 2, bentonite had distinctive spectra with a relatively higher intensity value. This result may be due to the high crystallinity components in bentonite, as previously stated in section 3.1. The IR spectrum of bentonite also exhibited a zeolite A structure (related to vibrations of the double four-membered ring), which was observed in 550 cm^{-1} (Król et al., 2016). The observed zeolitic structure in bentonite can be associated with a nacrite and lazurite mineral, which is classified as a tektosilicate mineral with 3D Si-Al frameworks (Hassan et al., 1985). Figure 2 also provides information on geopolymerization in each sample. The sharp peak of bentonite at 1023 cm^{-1} was shifted and broadened due to dissolution of crystalline materials forming geopolymer precursors. During hydrolysis reactions, the Al species were also simultaneously incorporated into the silicate structure (Hajimohammadi et al., 2010). The broadening of bentonite in the range of 900–1300 cm^{-1} indicates an amorphization of aluminate mineral structures in bentonite (Fernández-Jiménez and Palomo, 2005). Simultaneously, the geopolymer peak grew at about 1037 cm^{-1} . These bands indicate the existence of asymmetric vibration of Si-O-Al in tetrahedral coordination.

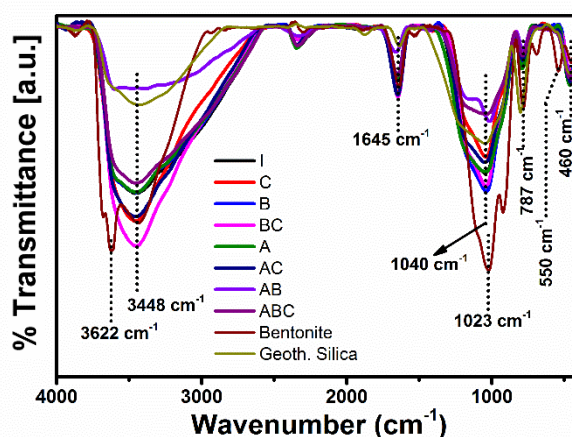


Figure 2 FTIR spectra of geothermal silica, bentonite and geopolymer specimens.

The effect of the particular variable in chemical bonds is shown in Figures 3a–3c with sample BC as a benchmark for other samples, as it has the highest compressive strength of

the other samples. The dramatic difference in the height of the absorbance peak is shown in Figure 3a. Figure 3a depicts the effect of silica content in samples with the run code of BC and ABC. It was found that the BC sample had a higher intensity peak at 1040 cm^{-1} than the ABC sample. A lower intensity peak of the ABC sample can be attributed to the lack of Al content as an essential element in geopolymer formation. The effect of different NaOH molarity in the geopolymer bond is presented in Figure 3b. A high concentration of NaOH solution provided a higher dissolution rate of raw materials into monomeric Si and Al. Furthermore, the monomers reacted to form aluminosilicate gel. The geopolymer sample with the run code of C had a lower concentration of aluminosilicates structures (zeolitic and geopolymeric structure) compared with the BC sample, due to the usage of a lower NaOH concentration (8 M). Figure 3c presents the influence of curing temperature in the development of the geopolymer bonds and zeolitic phase in samples B and BC. A higher curing temperature accelerated the polymerization process. At the macroscopic level, a higher compressive strength was notably observed (Table 3).

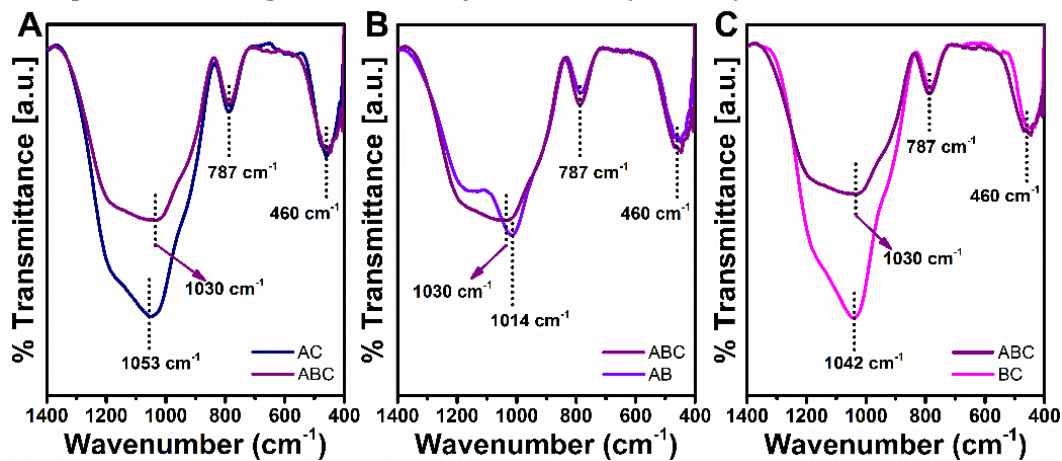


Figure 3 Enlarged FTIR spectra for selected geopolymer samples showing the effect of: (a) silica content (BC: 130 g/10 M/80°C; ABC: 140 g/10 M/80°C); (b) NaOH molarity BC: 130 g/10 M/80°C; C: 130 g/8 M/80°C); and (c) curing temperature (BC: 130 g/10 M/80°C; B: 130 g/10 M/60°C)

3.3. Microstructure Analysis using SEM-EDS

The SEM images of geopolymer samples (ABC, BC, B, and C) are shown in Figure 4. The microstructure of each sample can be evidence of a particular effect and is related to their compressive strength properties. In this study, the resulting morphologies of the geopolymer samples were compared. Furthermore, EDS observation for those samples was conducted to analyze key elemental distribution. Based on Figure 4, the resulting morphologies were relatively similar. The geopolymer layer, unreacted particles (pointed by white arrows), and cracks were found in the SEM images. As expected, a higher curing temperature led to an increase in the strength of the material, which is indicated by compact layer structures. In the early state, silicate and aluminate species reacted and formed a polymeric chain through a polycondensation reaction. Hence, the mixture produced water and looked like a gelatinous or thick-slurry paste. To remove the water and accelerate geopolymerization, the samples were cured at 60°C and 80°C. Figure 4 shows that samples BC (Figure 4b) and C (Figure 4d) had a denser microstructure than sample B (Figure 4c). This indicates that the geopolymerization process on samples BC and C occurred at a higher rate of reaction than sample B. Due to a lower rate of reaction, larger microcracks were formed on sample B, which decreased their compressive strength properties. These findings are consistent with previously reported parameters for metakaolinite-based geopolymers (Bing-hui et al., 2014).

Elemental mapping images using EDS for BC and C samples are shown in Figure 5. These figures provide valuable information on the elemental distribution of geopolymer samples. The elemental distribution can be an indicator of the formation of the aluminosilicate phase. The figures show the occurrence of silicon and alumina species. Each element was relatively well distributed in the geopolymer binder for sample BC (Figures 5a and 5b). For sample C, Figure 5d shows a large Si element cluster (pointed by white arrow). This cluster indicates the unreacted phase due to insufficient amounts of hydroxide ions for Si-Al mineral dissolutions. The EDS spectra of sample BC (Figure 5c) show a relatively higher intensity for the Na element compared to sample C (Figure 5f). This is a convincing evidence that a sufficient amount of hydroxide ions from NaOH is required to produce silica and aluminate species in geopolymerization. A higher amount of Na element contributes to the sodium aluminosilicate hydrates (N-A-S-H) gel species formation. This gel species significantly contributes to producing a dense and more compact geopolymer layer (Deb et al., 2015).

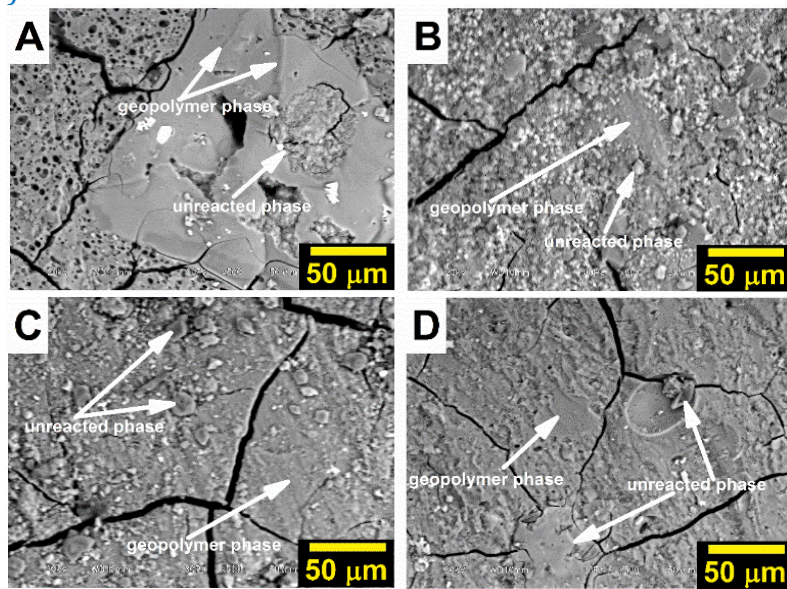


Figure 4 SEM images of geopolymer samples with the run code of: (a) ABC: 140 g/10 M/80°C; (b) BC: 130 g/10 M/80°C; (c) B: 130 g/10 M/60°C; and (d) C: 130 g/8 M/80°C

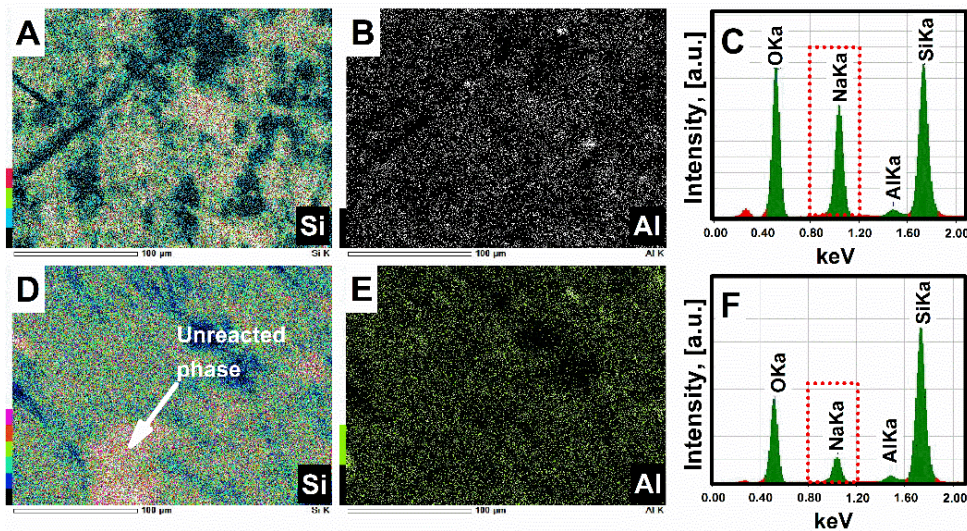


Figure 5 Elemental mapping images of Si (A and D), Al (B and E), and EDS spectra (C and F) for geopolymer samples with the run code of BC (First row) and C (second row). (Scale bar: 100 μm)

3.4. Statistical Analysis and Fitting of Polynomial Equation

A two-level factorial design was employed to achieve the optimum compressive strength of the geopolymer material. The linear fitting technique was employed to predict the fitness between theoretically calculated and measured values of the dependent variable (compressive strength). Table 3 displays the measured and predicted values of the compressive strength of the geopolymer samples. The second-order polynomial equation for expressing the empirical relationship between the dependent (compressive strength) and independent variables (silica content, NaOH molarity, and curing temperature) was constructed as follows:

$$\text{Compressive strength (MPa)} = 50.32 - 0.2747X_1 - 2.316X_2 - 0.4234X_3 + 0.00575X_1X_2 + 0.002575X_1X_3 + 0.01988X_2X_3 \quad (2)$$

Table 3 The experimental and calculated values of the geopolymer compressive strength

| Run code | X ₁ | X ₂ | X ₃ | Exp. Values of Comp. Strength (MPa) | Pred. Values of Comp. Strength (MPa) |
|----------|----------------|----------------|----------------|-------------------------------------|--------------------------------------|
| ABC | 140 | 10 | 80 | 7.60 | 7.62 |
| AB | 140 | 10 | 60 | 4.91 | 4.91 |
| AC | 140 | 8 | 80 | 7.47 | 7.47 |
| A | 140 | 8 | 60 | 5.52 | 5.54 |
| BC | 130 | 10 | 80 | 7.74 | 7.74 |
| B | 130 | 10 | 60 | 5.51 | 5.53 |
| C | 130 | 8 | 80 | 7.67 | 7.69 |
| I | 130 | 8 | 60 | 6.29 | 6.28 |

To ensure the adequacy of the model, it is important to perform an analysis of variance (ANOVA) test. This statistical technique can be used to separate the total variation into its component parts for model parameter testing (Montgomery, 2013). Furthermore, the effect of single variable and combined variables were tested using F-test and P-value to assess which specific effects are statistically significant. ANOVA analysis results are presented in Table 4 and showed that the p-value of the proposed model was statistically significant, as the p-value (0.024) was lower than the α value (0.05). The linear effect silica content and curing temperature had a p-value of 0.041 and 0.008, respectively. These values imply that silica content and curing temperature were also statistically significant on the geopolymer's compressive strength. On the contrary, the interaction terms had no significant effect due to their higher p-value.

Table 4 Results of ANOVA analysis

| Source | Effect | Coefficient estimate | SE coef. | DF | Adj. Sum of square | Adj. Mean square | F-value | P-value |
|--------------------------------|---------|----------------------|----------------|--------|--------------------|------------------|---------|---------|
| Model | | | | 6 | 9.5055 | 1.5842 | 1047.45 | 0.024 |
| Linear | | | | 3 | 9.0503 | 3.0167 | 1994.56 | 0.016 |
| X ₁ | -0.4275 | -0.2138 | 0.0138 | 1 | 0.3655 | 0.3655 | 241.66 | 0.041 |
| X ₂ | -0.2975 | -0.1487 | 0.0138 | 1 | 0.1770 | 0.1770 | 117.03 | 0.059 |
| X ₃ | 2.0625 | 1.0312 | 0.0138 | 1 | 8.5078 | 8.5078 | 5625.00 | 0.008 |
| 2-Way Interaction | | | | 3 | 0.4552 | 0.1517 | 100.33 | 0.073 |
| X ₁ *X ₂ | 0.0575 | 0.0288 | 0.0138 | 1 | 0.0066 | 0.0066 | 4.37 | 0.284 |
| X ₁ *X ₃ | 0.2575 | 0.1287 | 0.0138 | 1 | 0.1326 | 0.1326 | 87.68 | 0.068 |
| X ₂ *X ₃ | 0.3975 | 0.1987 | 0.0138 | 1 | 0.3160 | 0.3160 | 208.93 | 0.044 |
| Error | | | | 1 | 0.0015 | 0.0015 | | |
| Total | | | | 7 | 9.5070 | | | |
| R-square | 99.89% | | R-square (adj) | 99.89% | | | | |

The validity of the model's fitness can be predicted by comparing the measured and predicted data of the compressive strength. In Figure 6, the data points followed the same trend as a straight line and were sufficiently correlated. The model's adequacy and fitness can be quantified by the coefficient of correlation (R^2). The R^2 was 99.89%, indicating that 99% of the measured data matched the model. Thus, the proposed model in this study was able to correlate the independent variables (silica content, NaOH molarity, and curing temperature) with a compressive strength of geopolymer samples.

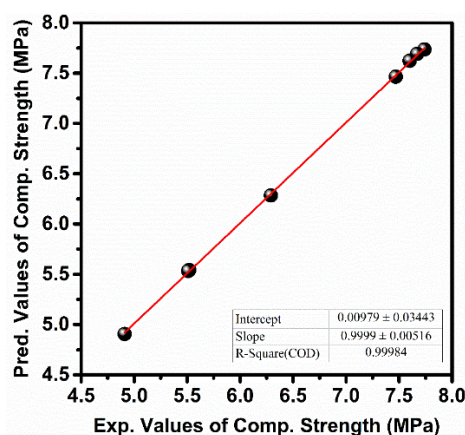


Figure 6 Linear fitting of data points obtained from experiments and predicted values of compressive strength.

3.5. Effect of Independent Variables on Compressive Strength

Geopolymerization using geothermal silica and bentonite has been previously studied with respect to the independent variables. The goal of this study was to optimize the independent variables to achieve the material with the best compressive strength. To identify the effect of combined variables, contour plots were constructed using Minitab software. The contour plot describes the effect of two combined variables, as presented in Figures 7a-7c. The combined effect of silica content and NaOH molarity on compressive strength is illustrated by Figure 7a. The compressive strength of the geopolymer was sensitive to the change in silica content and NaOH molarity. In Figure 7a, the compressive strength values increased with decreasing silica content and NaOH molarity. The maximum compressive strength could be obtained using 130 g of silica content and 8 M of NaOH molarity. Figure 7b presents the effect of NaOH molarity and curing temperature on compressive strength values. Both variables in Figure 7b had a significant effect on the compressive strength. The compressive strength increased with increasing NaOH molarity and curing temperature. The contour plot in Figure 7a suggests that the maximum compressive strength could be achieved at 10 M of NaOH molarity and 80°C of curing temperature. The contour plot in Figure 7c exhibits the interactive effect of silica content and curing temperature on geopolymer strength. There was an interaction between silica content and curing temperature, which influences the material's strength. A lower value of silica content led to higher compressive strength. On the contrary, higher compressive strength can be attained by a higher curing temperature. To achieve the highest compressive strength, we suggest that the geopolymer should be produced using 130 g silica content and 80°C curing temperature.

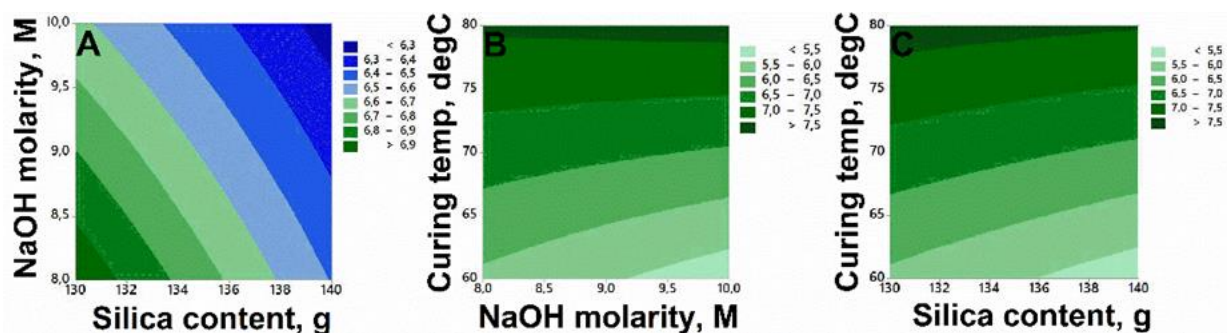


Figure 7 2D Contour plots showing the relation of combined variables with compressive strength

Optimum variables in this study were deduced to attain a maximum compressive strength of the geopolymer. The possible result of the numerical optimization is an optimum value of the response located in the range of used variables. To optimize the compressive strength of geopolymer, the parameters (1) silica content (130–140 g); (2) NaOH molarity (8–10 M); and (3) curing temperature (60–80°C) were set to achieve the best properties, indicated by high desirability value (0 for completely undesirable response, 1 for fully desired response). By using this method, the optimized variables were obtained, which was indicated as 130 g silica content, 10 M NaOH and 80°C curing temperature, to obtain an optimized compressive strength of 7.73 MPa with a desirability value of 0.99.

4. Conclusions

A geopolymer has been successfully produced by using geothermal silica and bentonite. Its characterization using FTIR and SEM-EDS showed that the aluminosilicate structure was formed in all prepared samples. The effects of combined variables have been studied and optimized using the RSM technique. The geopolymerization rate can be accelerated using the lower level of geothermal silica and the high level of NaOH molarity and curing temperature. Based on optimization studies, the coefficient of correlation (R^2) obtained was 99.89%. The optimum formulation (desirability value = 0.99) for geopolymer production from geothermal silica and bentonite is using 136 g of silica content, 10 M of NaOH molarity, and 80°C of curing temperature. At the optimum condition, the compressive strength was 7.73 MPa.

Acknowledgements

This research was financially supported by AUN-SEED-Net JICA Common Regional Issues (CRC) 2016. The authors also acknowledge PT. Geodipa Energy, Dieng for providing geothermal silica, Unconventional Georesources Research Center, UGM and LIPI' Science Services for Research Laboratories for supporting this research.

References

- Alshaaer, M., 2013. Two-Phase Geopolymerization of Kaolinite-Based Geopolymers. *Applied Clay Science*, Volume 86, pp. 162–168
- Ashadi, H.W., Aprilando, B.A., Astutiningsih, S., 2015. Effects of Steel Slag Substitution in Geopolymer Concrete on Compressive Strength and Corrosion Rate of Steel Reinforcement in Seawater and an Acid Rain Environment. *International Journal of Technology*, Volume 6(2), pp. 227–235

- Bezerra, M.A., Santelli, R.E., Oliveira, E.P., Villar, L.S., Escalera, L.A., 2008. Response Surface Methodology (RSM) as a Tool for Optimization in Analytical Chemistry. *Talanta*, Volume 76(5), pp. 965–977
- Bing-hui, M., Zhu, H., Xue-min, C., Yan, H., Si-yu, G., 2014. Effect of Curing Temperature on Geopolymerization of Metakaolin-Based Geopolymers. *Applied Clay Science*, Volume 99, pp. 144–148
- Deb, P.S., Sarker, P.K., Barbhuiya, S., 2015. Effects of Nano-Silica on the Strength Development of Geopolymer Cured at Room Temperature. *Construction and Building Materials*, Volume 101(1), pp. 675–683
- Dhakal, M., Kupwade-Patil, K., Allouche, E.N., la Baume Johnson, C.C., Ham, K., 2014. *Optimization and Characterization of Geopolymer Mortars using Response Surface Methodology*. In: *Developments in Strategic Materials and Computational Design IV*, Kriven, W. M., Wang, J., Zhou, Y., Gyekenyesi, A. L. (Eds.), John Wiley and Sons, pp. 135–149
- Dhaneswara, D., Fatriansyah, J.F., Situmorang, F.W., Haqoh, A.N., 2020. Synthesis of Amorphous Silica from Rice Husk Ash: Comparing HCl and CH₃COOH Acidification Methods and Various Alkaline Concentrations. *International Journal of Technology*, Volume 11(1), pp. 200–208
- Duxson, P., Fernández-Jiménez, A., Provis, J.L., Luckey, G.C., Palomo, A., van Deventer, J.S.J., 2007. Geopolymer Technology: The Current State of the Art. *Journal of Material Science*, Volume 42, pp. 2917–2933
- Ferdana, A.D., Petrus, H.T.B.M., Bendiyasa, I.M., Prijambada, I.D., Hamada, F., Sachiko, T., 2018, Optimization of Gold Ore Sumbawa Separation using Gravity Method: Shaking Table. *AIP Conference Proceedings*, Volume 1945, p. 020070
- Fernández-Jiménez, A., Palomo, A., 2005. Mid-Infrared Spectroscopic Studies of Alkali-Activated Fly Ash Structure. *Microporous and Mesoporous Materials*, Volume 86(1-3), pp. 207–214
- Gao, Y., Xu, J., Luo, X., Zhu, J., Nie, L., 2016. Experiment Research on Mix Design and Early Mechanical Performance of Alkali-Activated Slag using Response Surface Methodology (RSM). *Ceramic International*, Volume 42(10), pp. 11666–11673
- Gomez-Zamorano, L.Y., Vega-Cordero, E., Struble, L., 2016, Composite Geopolymers of Metakaolin and Geothermal Nanosilica Waste. *Construction and Building Materials*, Volume 115, pp. 269–276
- Hajimohammadi, A., Provis, J.L., van Deventer, J.S.J., 2008. One-Part Geopolymer Mixes from Geothermal Silica and Sodium Aluminate. *Industrial & Engineering Chemistry Research*, Volume 47(23), pp. 9396–9405
- Hajimohammadi, A., Provis, J.L., van Deventer, J.S.J., 2010. Effect of Alumina Release Rate on the Mechanism of Geopolymer Gel Formation. *Chemistry of Materials*, Volume 22(18), pp. 5199–5208
- Hairi, S.N.M., Jameson, G.N.L., Rogers, J.J., MacKenzie, K.J.D., 2015. Synthesis and Properties of Inorganic Polymers (Geopolymers) Derived from Bayer Process Residue (Red Mud) And Bauxite. *Journal of Material Science*, Volume 50, pp. 7713–7724
- Hassan, I., Peterson, R.C., Grundy, H.D., 1985. The Structure of Lazurite, Ideally Na₆Ca₂(Al₆Si₆O₂₄)S₂, a Member of the Sodalite Group. *Acta Crystallographica Section C*, Volume 41, pp. 827–832
- Heath, A., Paine, K., McManus, M., 2014. Minimising the Global Warming Potential of Clay-Based Geopolymers. *Journal of Cleaner Production*, Volume 78, pp. 75–83

- Januardi, J., Widodo, E., 2020, Response Surface Methodology of Dual-Channel Green Supply-Chain Pricing Model by Considering Uncertainty. *Supply Chain Forum: An International Journal*, DOI: 10.1080/16258312.2020.1788904, pp. 1–12
- Król, M., Minkiewicz, J., Mozgawa, W., 2016. IR Spectroscopy Studies of Zeolites in Geopolymeric Materials Derived from Kaolinite. *Journal of Molecular Structure*, Volume 1126, pp. 200–206
- Mohammed, B.S., Khed, V.C., Nuruddin, M.F., 2018. Rubbercrete Mixture Optimization using Response Surface Methodology. *Journal Cleaner Production*, Volume 171, pp. 1605–1621
- Montgomery, D.C., 2013. *Design and Analysis of Experiments* 8th ed., New Jersey: John Wiley & Sons
- Nurjaya, D.M., Astutiningsih, S., Zulfia, A., 2015, Thermal Effect on Flexural Strength of Geopolymer Matrix Composite with Alumina and Wollastonite as Fillers. *International Journal of Technology*, Volume 6(3), pp. 462–470
- Olvianas, M., Najmina, M., Prihardana, B.S.L., Sutapa, F.A.K.G.P., Nurhayati, A., Petrus, H.T.B.M., 2015. Study on the Geopolymerization of Geothermal Silica and Kaolinite. *Advanced Materials Research*, Volume 1112, pp. 528–532
- Perná, I., Hanzlíček, T., Šupová, M., 2014. The Identification of Geopolymer Affinity in Specific Cases of Clay Materials. *Applied Clay Science*, Volume 102, pp. 213–219
- Petrus, H.T.B.M., Hulu, J., Dalton, G.S.P., Malinda, E., Prakosa, R.A., 2016. Effect of Bentonite Addition on Geopolymer Concrete from Geothermal Silica. *Materials Science Forum*, Volume 841, pp. 7–15
- Petrus, H.T.B.M., Putra, A.E., Gustiana, H.S.A., Prasetya, A., Bendiyasa, I.M., Astuti, W., 2020, Gold Leaching from Printed Circuit Boards (PCBs) as one of the Urban Mine Resources using Thiosulphate: Optimization using Response Surface Methodology (RSM). In: IOP Conference Series: Materials Science and Engineering, Volume 778, pp. 012166
- Provis, J.L., Lukey, G.C., van Deventer, J.S.J., 2005. Do Geopolymers Actually Contain Nanocrystalline Zeolites? A Reexamination of Existing Results. *Chemistry of Materials*, Volume 17, pp. 3075–3085
- Skvara, F., Jilek, T., Kopecky, L., 2005. Geopolymer Material based on Fly Ash. *Ceramics-Silikáty*, Volume 49(3), pp. 195–204
- van Deventer, J.S.J., Provis, J.L., Duxson, P., Lukey, G.C., 2007. Reaction Mechanisms in the Geopolymeric Conversion of Inorganic Waste to Useful Products. *Journal of Hazardous Materials*, Volume 139(3), pp. 506–513
- Xua, H., van Deventer, J.S.J., 2003. Effect of Source Materials on Geopolymerization. *Industrial & Engineering Chemistry Research*, Volume 42(8) pp. 1698–1706
- Ye, N., Yang, J., Liang, S., Hu, Y., Hu, J., Xiao, B., Huang, Q., 2016, Synthesis and Strength Optimization of One-Part Geopolymer based on Red Mud. *Construction and Building Materials*, Volume 111, pp. 317–325
- Zhang, Z., Wang, H., Provis, J.L., 2012. Quantitative Study of the Reactivity of Fly Ash in Geopolymerization by FTIR. *Journal of Sustainable Cement-Based Materials*, Volume 1(4), pp. 154–166
- Şimşek, B., İç, Y.T., Şimşek, E.H., 2015. A RSM-Based Multi-Response Optimization Application for Determining Optimal Mix Proportions of Standard Ready-Mixed Concrete. *Arabian Journal for Science and Engineering*, Volume 41, pp. 1435–1450